Impaired intranuclear trafficking of Runx2 (AML3/CBFA1) transcription factors in breast cancer cells inhibits osteolysis *in vivo*

Amjad Javed*, George L. Barnes†, Jitesh Pratap*, Tomasz Antkowiak*, Louis C. Gerstenfeld†, Andre J. van Wijnen*, Janet L. Stein*, Jane B. Lian*, and Gary S. Stein*‡

*Department of Cell Biology and Cancer Center, University of Massachusetts Medical School, 55 Lake Avenue North, Worcester, MA 01655; and †Orthopaedic Reseach Laboratory, Department of Orthopaedic Surgery, Boston University Medical Center, 715 Albany Street, Boston, MA 02118

Communicated by Sheldon Penman, Massachusetts Institute of Technology, Brookline, MA, December 17, 2004 (received for review October 20, 2004)

Runx transcription factors comprise a family of proteins that are essential for organogenesis. A unique nuclear matrix-targeting signal in the C terminus directs these factors to their appropriate subnuclear domains. At these sites, they interact with coregulatory proteins and target genes. We have previously shown that aberrant expression of the Runx2 DNA binding domain in metastatic breast cancer cells can prevent production of osteolytic lesions in bone. Here, we show that proper Runx2 subnuclear targeting is required for osteolysis. We have identified point mutations of the Runx2 nuclear matrix-targeting signal sequence that impair its targeting to nuclear matrix sites. These mutations block the invasive and osteolytic properties of MDA-MB-231 breast cancer cells *in vivo*. Cell lines expressing this Runx2 mutant protein inhibit the osteogenic properties of bone marrow stromal cells in coculture assays. The mutant breast cancer cells also exhibit reduced invasiveness *in vitro* and do not express genes involved in invasion and angiogenesis (VEGF and MMP13). Our findings suggest that fidelity of Runx2 intranuclear organization is necessary for expression of target genes that mediate the osteolytic activity of metastatic breast cancer cells.

gene expression | intranuclear organization | nuclear matrix

Runx (AML/CBFA/PEBP2) transcription factors are tissue-specific regulatory proteins that are involved in the control of hematopoiesis (Runx1/AML1), osteogenesis (Runx2/AML3), and neural and gastrointestinal cell differentiation (Runx3/AML2) (1–3). Translocations or mutations of Runx1 results in leukemogenesis (4), whereas mutations of Runx2 and Runx3 lead to skeletal disease (5) and stomach cancer (3), respectively. The Runx transcription factors function as scaffolds for interaction with various coregulatory proteins. These complexes interact in a combinatorial fashion to regulate gene expression. Furthermore, Runx proteins are focally localized within the nucleus. The subnuclear localization of Runx proteins requires at least two trafficking signals; one signal supports nuclear import (nuclear localization signals) and the other signal is required for residency in nuclear matrix-associated regulatory domains (nuclear matrix-targeting signal; NMTS) (6–9). The role of Runx proteins in both gene expression and nuclear structure is a reflection of their modular organization. The N terminus binds specific DNA sequences, whereas the C-terminal domain interacts with coregulatory factors and associates with the nuclear matrix (10–13). During tissue differentiation, Runx proteins form stage-specific complexes with subsets of coactivators (14–16), corepressors (17–19), and factors that are end points of key signaling cascades (20, 21). These multimeric complexes are organized in punctuate subnuclear foci that constitute nuclear microenvironments (22).

The critical role of Runx2 in osteogenesis has provided a model for investigating the importance of subnuclear localization for tissue differentiation. Mice homozygous for Runx2 protein lacking the C terminus that includes the NMTS do not form bone because of maturational arrest of osteoblasts (23). In a manner analogous to the human bone disorder cleidocranial dysplasia, heterozygous mice do not develop clavicles. These phenotypes are indistinguishable from those of the Runx2 homozygous and heterozygous null mutants (2). Thus, the NMTS and its role in integration of osteogenic regulatory signals at sites within the nucleus are critical determinants for Runx2 biological function (20, 24, 25). Analogously, mice expressing Runx1 protein mutated at the C terminus exhibit a phenotype indistinguishable from that of mice with an ablated Runx1 gene (26). These results suggest that the correct subnuclear localization of Runx factors and their association with coregulatory proteins are essential for control of Runx-responsive genes involved in tissue differentiation and embryonic development.

It is widely recognized that breast cancer cells preferentially metastasize to bone (27, 28). The expression of Runx2 and other osteoblast-related genes by breast and prostate cancer cells has been well documented (29–31). These gene products are thought to facilitate interactions between the tumors and the bone microenvironment. We have reported (29) that inhibiting Runx2 activity abolishes the ability of breast cancer cells to form osteolytic lesions *in vivo*. Thus, these lesions serve as an assay for Runx2 function. In this study, we demonstrate by selective mutation that correct intranuclear trafficking of Runx2 is required for bone phenotypic gene expression. Furthermore, perturbation of Runx2 subnuclear localization in breast cancer cells inhibits formation of osteolytic lesions in bone *in vivo*.

Materials and Methods

Site-Directed Mutagenesis and Expression Plasmid. Hemagglutinin (HA)-tagged NMTS mutant Runx2 (R398A and Y428A) was generated by using a site-directed mutagenesis kit (Stratagene). To incorporate the 2-bp substitution mutation that changes arginine at position 398 to alanine, we synthesized complementary oligonucleotides. Y428A mutant Runx2 plasmid (20) was amplified by PCR using forward 5′-GCTTCTCCAACCCAGCAATGCACTAC-3′ and reverse 5′-GTAGTGCATTGCTGGGTTGGAGAAGC-3′ primers. Amplicons with both mutations (R398A and Y428A) were digested with *Dpn*I and transformed into chemically modified *Escherichia coli* competent cells. To avoid nonspecific mutations, the positive clones identified by sequence analysis were digested with *Apa*I–*Xho*I, and the released fragment was swapped into the HA-tagged Runx2 plasmid. The mouse Cbfβ coding region was amplified by PCR using the forward 5′-GCGGATCCATGC-CGCGCGTC-3′ and reverse 5′-CGAATTCCTAGGGTCT-TGC-3′ primers. PCR product was digested with *Bam*HI and

Abbreviations: WC, whole cell; NMTS, nuclear matrix targeting signal; HA, hemagglutinin; NMIF, nuclear matrix intermediate filament; BMSC, bone marrow stromal cell; RPA, RNase protection analysis; CSK, cytoskeleton.

‡To whom correspondence should be addressed. E-mail: gary.stein@umassmed.edu.

© 2005 by The National Academy of Sciences of the USA

www.pnas.org/cgi/doi/10.1073/pnas.0409121102

*Eco*RI and cloned into similarly digested pcDNA3.1 vector. Expression vectors for Msx2, TLE1, HA-Runx2, and Smad1 have been reported (14, 17, 20).

Transient Transfection and Coimmunoprecipitations. HeLa cells were cotransfected with 5 μg of WT or R398A and Y428A mutant Runx2, as well as with Msx2, TLE1, Smad1, or Cbfβ expression plasmids by using SuperFect reagent (Qiagen, Valencia, CA). BMP2 treatments (200 ng/ml) were carried out 4 h later for Smad-transfected plates only. Cells were harvested 24 h later and lysed by sonication. Protein complexes were precipitated with a Runx2 polyclonal Ab (Santa Cruz Biotechnology; 3 μg/IP). Conditions for coimmunoprecipitations were essentially as described (17). Western blots were sequentially probed with mAbs against Flag epitope (1:5,000; Sigma–Aldrich), Xpress epitope (1:5,000; Invitrogen) and Runx2 (1:3,000; ref. 21).

Generation of Stable Cell Lines. Stable MDA-MB-231 human breast adenocarcinoma cell lines were generated that express the empty vector pcDNA 3.1 (Invitrogen), HA-tagged WT, or the R398A and Y428A mutant Runx2 as described (15, 29). Cells were transfected with Lipofectamine reagent according to manufacturer's recommendations (Invitrogen) and selected based on neomycin (G418) resistance.

Subcellular Fractionation and Western Blot Analysis. Breast cancer stable cell lines expressing WT or R398A and Y428A mutant Runx2 were harvested at confluency in PBS containing 25 μM MG132 and Complete protease inhibitor (Roche Molecular Biochemicals). Whole-cell (WC) pellets were lysed in 300 μl of lysis buffer (25 mM Tris·Cl, pH 7.5/150 mM NaCl/1 mM Na_2·EDTA/1 mM EGTA/1% Triton X-100/1% Nonidet P-40/25 μM MG132/protease inhibitor mixture). Biochemical fractionation was carried out on a separate cell pellet essentially as described in refs. 8 and 32. For Western blotting, equal fraction volumes (30 μl) were resolved on 10% SDS/PAGE. Blots were probed with HA mAb, stripped mildly, and reprobed with Ab against Lamin B (1:5,000; Santa Cruz Biotechnology).

Immunofluorescence Microscopy. WT and mutant Runx2 MDA-stable cells were processed for WC or nuclear matrix intermediate filament (NMIF) preparations, as described (14). Cells were incubated with 1:3,000 dilution of mouse HA mAb (Santa Cruz Biotechnology) at 37°C for 1 h, followed by four washes with PBSA (0.5% BSA in PBS), and then stained with 1:1,000 dilution of anti-mouse Alexa 488 secondary Ab (Molecular Probes). After washing with PBSA, DAPI staining (0.02 mg/ml) was performed for 5 min on ice. Cells were then mounted with VECTASHIELD mounting media (Vector Laboratories). Digital imaging of cells was performed by using an Axioplan 2 microscope (Zeiss) equipped with fluorescence filters and a charge-coupled device camera (Hamamatsu, Middlesex, NJ) and interfaced with the MetaMorph Imaging System (Universal Imaging, West Chester, PA).

Osteogenic Superarray and Real-Time Quantitative PCR. Total RNA from parental, WT, and mutant Runx2 stable MDA-MB-231 cell lines was isolated by using Trizol reagent according to the manufacturer's instructions. Expression levels were assessed with 5 μg of total RNA by using the human osteogenesis cDNA expression array kit (SuperArray Bioscience, Frederick, MD) according to the manufacturer's protocol. Signal intensities of each marker gene were normalized to GAPDH values and data plotted by using DCHIP, a DNA-chip analysis software (33). The reverse transcriptase reaction was performed on total RNA by using the SuperScript II kit according to the manufacturer's instructions. Real-time PCR analysis was performed to confirm expression levels of MMP13 [5′-TCTGAACTGGGTCTTCCAAAA-3′ (forward) and 5′-GCATCTACTTTATCACCAATTCCT-3′ (reverse)] and VEGF [5′-TCTTCAAGCCATCCTGTGTG-3′ (forward) and 5′-GCGAGTCTGTGTTTTTGCAG-3′ (reverse)] by using an ABI machine and PRISM software (Applied Biosystems).

Cell-Invasion Assay. Cells were analyzed for migration potential on Matrigel (BD Biosciences) according to the manufacturer's protocols. Briefly, 1×10^5 cells per ml were added to control inserts or inserts containing Matrigel in serum-free medium. The lower chamber contained medium with 5% FBS. Cells were allowed to migrate for 20–22 h at 37°C. Nonmigrated cells were removed by scraping the top filter, and the migrated cells were stained with HEMA 3 kit (Fisher Scientific). Each filter was counted for cells in at least 10 random fields and represented as percentage of migration.

Preparation of Marrow Stromal Cells. Bone marrow stromal cell (BMSC) cultures were generated as described (29, 34, 35). At 5 days after initial plating, 5,000 human breast cancer cells (MDA-MB-231or R398A and Y428A mutant Runx2 stable line) were added to the cultures. Cultures were maintained in α-modified MEM containing 10% FBS, penicillin–streptomycin, 10^{-8} M dexamethasone, 50 μg/ml ascorbic acid and 8 mM β-glycerol phosphate with feeding every 48 h until harvest at 21 days. All media and supplements were purchased from GIBCO and Invitrogen.

RNase Protection Analysis (RPA). Total RNA was isolated from control and BMSC cocultures by using Trizol reagent as described

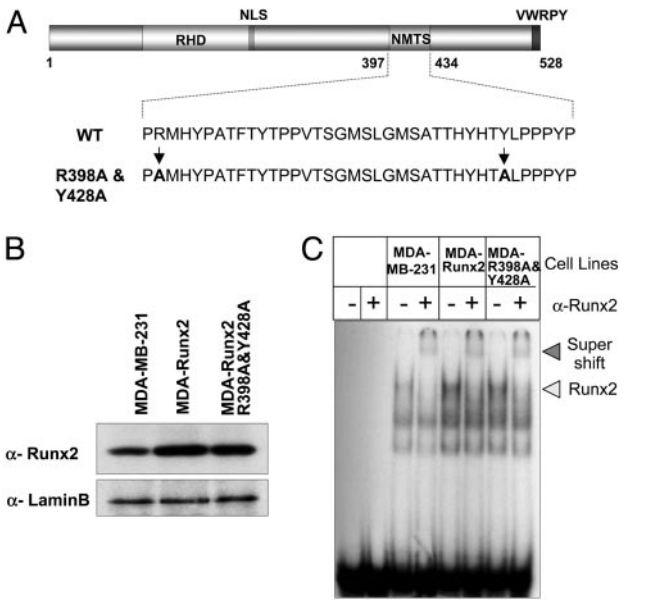

Fig. 1. WT and R398A and Y428A mutant Runx2 proteins are expressed in MDA-MB-231 stable cells and exhibit similar DNA binding activity. (*A*) Schematic representation of the mouse Runx2 protein with key domains highlighted (RHD, DNA binding *runt* homology domain; NLS, nuclear localization signal; NMTS; and VWRPY, a penta-peptide motif conserved among Runx factors). At the bottom, the 38 amino-acids (397–434) that constitute the NMTS are shown. Arginine and tyrosine at positions 398 and 428, respectively, were mutated to alanine. (*B*) MDA-MB-231 breast cancer cells were stably transfected with either WT or R398A and Y428A mutant Runx2 expression plasmids. Cell lysates from parental and stable lines were resolved in 10% SDS/PAGE, and Western blots were probed with mouse Runx2 mAb (44). Lamin B antigen is shown as a loading control. (*C*) Electrophoretic mobility shift analysis of Runx2 DNA binding activity from breast cancer lines. Nuclear extracts were isolated from the indicated cell lines as described (18). Runx consensus oligonucleotide used as probe was mixed with 10 μg of nuclear extract in the presence (+) or absence (−) of Runx2 Ab. Arrowhead indicates the Runx2–DNA complex.

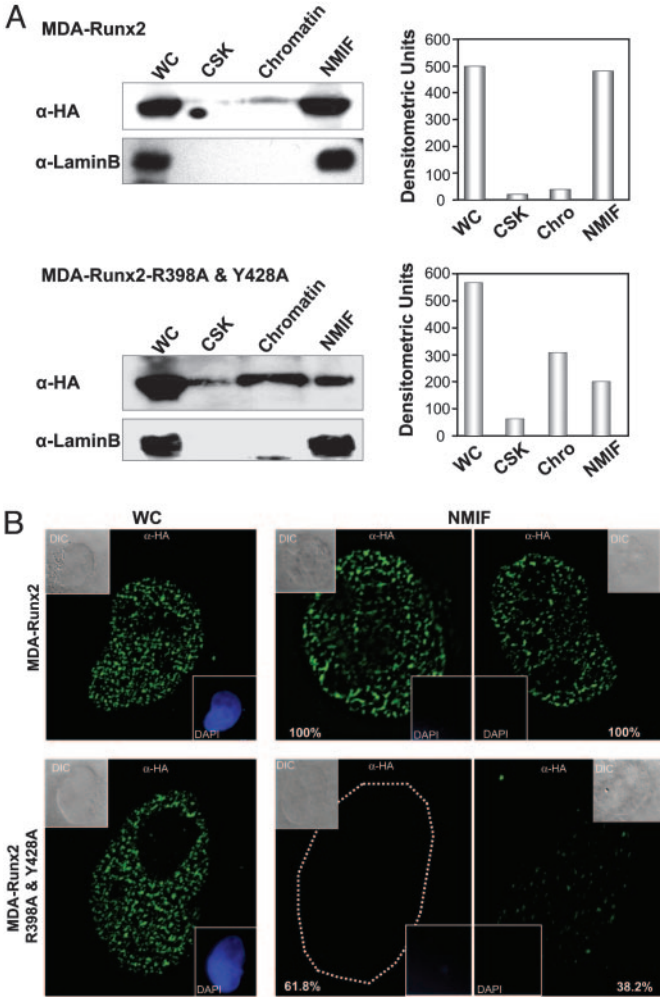

Fig. 2. Paired mutation of R398A and Y428A in Runx2 protein results in loss of nuclear matrix association in breast cancer cells. (*A*) Biochemical fractionation of breast cancer lines expressing WT or targeting-deficient Runx2 mutant protein. Harvested cell pellets were subjected to high-salt and detergent extraction to isolate CSK, chromatin, and NMIF fractions, as described in *Materials and Methods*. Equal fraction volumes based on cell equivalence were resolved in 10% SDS/PAGE, and membranes were probed with mouse HA mAb to detect Runx2 protein (*Left*). Integrity of subcellular fractions is confirmed by Lamin B, a marker for nuclear matrix. *Right* shows graphic representations of densitometric quantitation of Western blotting signals. (*B*) *In situ* immunofluorescence microscopy of Runx2 proteins in breast cancer stable lines. Cells were cultured on gelatin-coated cover slips and processed as WC or extracted to reveal the NMIF. Two representative cells are shown for WT (*Upper*) and R398A and Y428A Runx2 mutant (*Lower*). Cells from four independent NMIF preparations were counted, and percentages of HA-stained cells are shown. *Insets* show differential interference contrast (DIC) or DAPI stained images of the cell. Removal of chromatin in the NMIF preparations is reflected by the absence of DAPI staining. Magnifications are ×100.

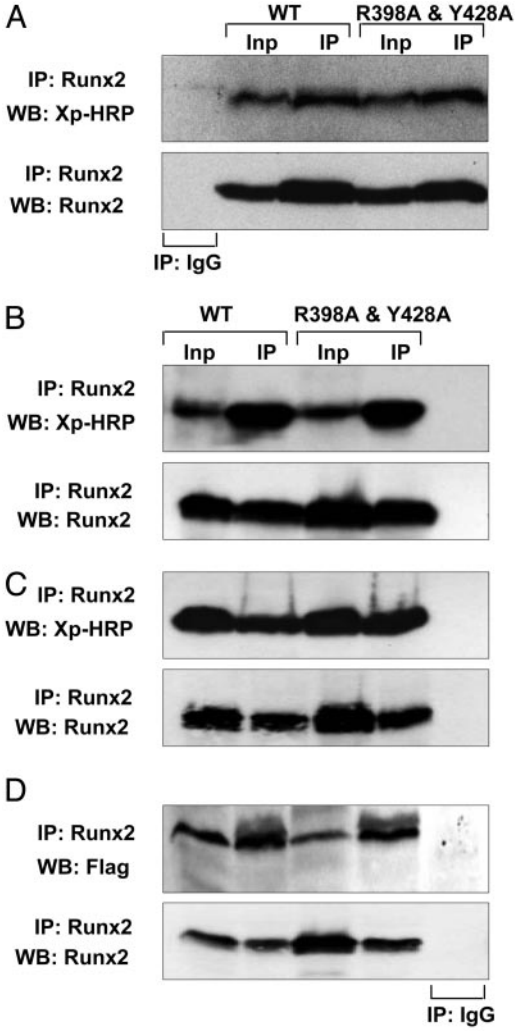

Fig. 3. Coregulatory protein interactions across the targeting-deficient Runx2 mutant protein are preserved. HeLa cells that do not express endogenous Runx proteins were transiently cotransfected with 5 μg of expression plasmid for WT or mutant Runx2 and coregulatory proteins: Groucho/TLE, a C terminus interacting protein (*A*); Cbfβ, an N terminus interacting protein (*B*); and two proteins that interact at the NMTS domain, Homeodomain Msx2 (*C*) and BMP2 mediator Smad1 (*D*). Cells were collected 24 h later, and immunoprecipitations were performed with Runx2 Ab. Immunocomplexes were resolved in 10–12% SDS/PAGE, and Western blots were probed as indicated. Inp, 10% of input control.

(29, 35). RPA was carried out by using commercially produced species-specific template sets and reagents from Pharmingen (BD Biosciences, Pharmingen). Band intensities were quantified and normalized by using an Alpha Innotech (San Leandro, CA) imaging system and associated CHEMIIMAGER 4000 software.

Surgical Protocols. Animal studies were conducted in accordance with approved Institutional Animal Care and Use Committee protocols and the National Institutes of Health Guide for the Care and Use of Laboratory Animals. Tibial intramedullary injections were carried out on isofluorane-anesthetized 4- to 6-week-old female SCID mice (The Jackson Laboratory) by using the technique described in refs. 29 and 36. The formation of osteolytic lesions in bones was assessed by radiography using a Faxitron MX-20 (Faxitron X-ray, Wheeling, IL). Bone radiographs were collected on X-Omat TL film (Kodak) using an exposure of 25 kV for 60 s.

Results and Discussion

Fidelity of Runx2 Intranuclear Trafficking Is Obligatory for Stringent Regulation of Bone Phenotypic Genes by Breast Cancer Cells. We showed that association with the nuclear matrix is necessary for Runx2 activity in breast cancer cells. We generated MDA-MB-231 stable cell lines containing either WT Runx2 or a point mutant defective in intranuclear targeting (TD mRunx2; Fig. 1*A*). This mutant has two amino acid substitutions (R398A and Y428A) and is strongly expressed. It enters the nucleus, where it shows normal DNA-binding activity (Fig. 1 *B* and *C*). Sepa-

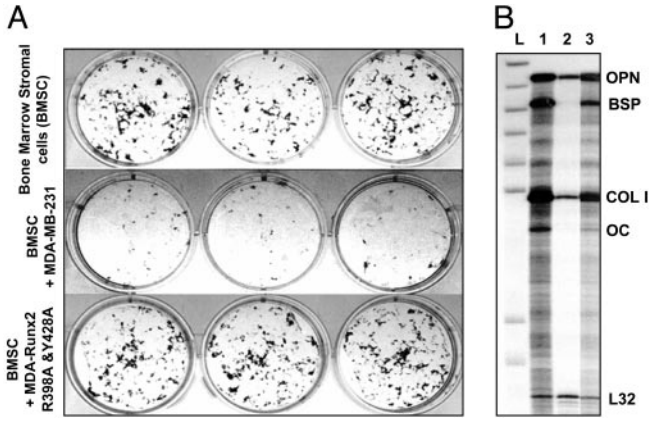

Fig. 4. Inhibition of bone marrow cell osteogenic differentiation by breast cancer cells is linked to subnuclear targeting of Runx2. Breast cancer cells (5,000) expressing WT or mutant Runx2 were added to 5-day-old murine BMSC cultures. Adherent cells were cultured for an additional 16 days in osteogenic medium (α-MEM supplemented with 10% FBS/10^{-8} M dexamethasone/50 μg/ml ascorbic acid/8 mM β-glycerol phosphate). (*A*) Plates were then stained by Von Kossa to reveal mineralized nodules. Three representative wells for each group are shown. (*B*) RPA of murine osteoblast marker gene expression in cocultures of mouse BMSC and human breast cancer cells. Total RNA was isolated from 20-day coculture cells and probed for osteoblastic markers as described in *Materials and Methods*. L, Undigested probe ladder; 1, BMSC alone; 2, BMSC cocultured with MDA-MB-231 cells; 3, BMSC cocultured with MDA cells stably expressing mutant Runx2. Key markers are osteopontin (OPN), bone sialoprotein (BSP), collagen type I (COL I), osteocalcin (OC), and ribosomal protein gene (L32) as an internal control.

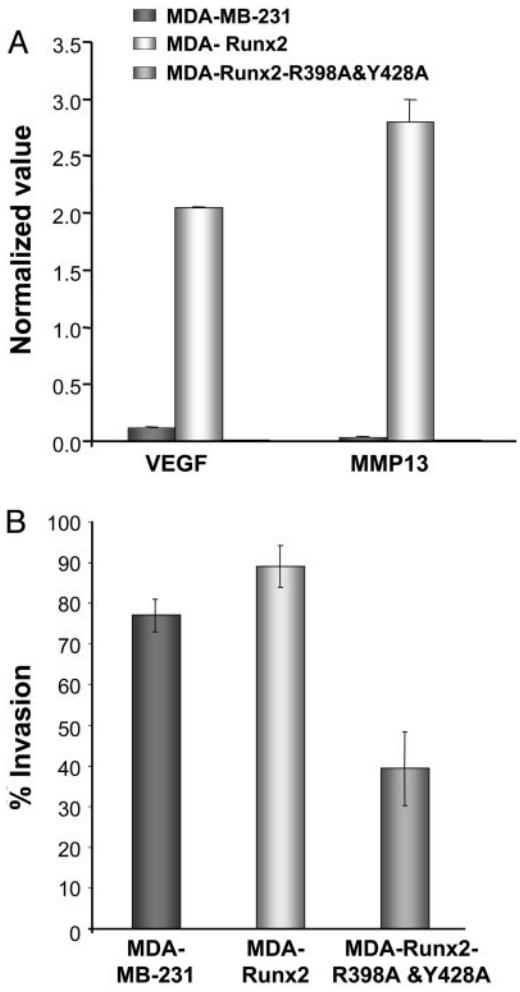

Fig. 5. Compromised Runx2 subnuclear targeting modifies phenotypic properties of the MDA breast cancer cells. RNA was isolated from MDA stable lines and osteogenic gene profiling assessed as described in *Materials and Methods*. (*A*) Validation of modified genes by quantitative RT-PCR. Changes in expression of two selected Runx2 responsive genes (VEGF and MMP13) were confirmed by real-time PCR. Values were normalized to GAPDH, which was equally expressed in the three cell lines. Significant induction of both genes was observed only in breast cancer stable lines expressing WT Runx2. (*B*) Runx2 regulates invasive potential of breast cancer cells. Cells from parental MDA-MB-231 or WT and mutant Runx2 stable breast cancer lines were plated in chambers as described. The Matrigel layer was then removed and the number of migrated cells counted. Data are plotted as percentage of cells that migrated through Matrigel in comparison with membrane control alone.

rating these cells into cytoskeleton (CSK), chromatin, and NMIF fractions shows that most WT Runx2 bound to the NMIF fraction. However, the mutant Runx2 protein exhibits altered subnuclear trafficking; it fails to bind to the NMIF and is located primarily in the chromatin fraction (Fig. 2*A*). Fig. 2*B* shows fluorescent images of extracted cells in which the WT Runx 2 remains bound to the isolated NMIF while targeting-deficient (TD-mRunx2) protein is completely removed.

Next, we showed that, aside from the loss of binding to the NMIF, the mutated TD-Runx2 protein retains interactions with Runx2 coregulatory factors. By using coimmunoprecipitation, we assessed protein–protein interactions with four critical coregulators that bind to different regions of Runx2 (Fig. 3). We selected the Cbfβ DNA binding partner that interacts with the N-terminal runt homology domain, the TLE/Groucho repressor protein that binds the C terminus, as well as the Msx2 homeodomain protein and the BMP responsive Smad1-signaling transducer that interact with the NMTS domain of Runx2. Similar to WT Runx2, the TD-Runx2 mutant protein interacts with each of the coregulatory factors (Fig. 3). Thus, the TD-mRunx2 retains normal DNA binding as well as interactions with corepressor and coactivator proteins. Therefore, any potential modification in the phenotype of the cells expressing this protein results from the loss of Runx2 association with the nuclear matrix and the resultant inability to organize transcriptional regulatory complexes in subnuclear foci.

Next, we tested the *in vitro* effects of the TD-mRunx2 in modifying osteogenic activity of the MDA-MB-231 parental breast cancer cell line by using an *in vitro* coculture assay. The human breast cancer cells were cultured in the presence of mouse marrow stromal cells, a source of osteoprogenitors that differentiate into mineralized bone nodules. We have previously shown that the parental MDA-MB-231 cell line, which expresses Runx2 (see Fig. 1*B*), inhibits formation of osteogenic colonies in this assay (Fig. 4*A*). In contrast, coculture with the TD-mRunx2 cell line fails to inhibit the osteogenic colony formation by the marrow stromal cells. Furthermore, the expression of several osteoblastic genes in the mouse stromal cells is inhibited by the parental breast cancer cells but not by cells expressing TD mutant Runx2 (compare lanes 2 and 3; Fig. 4*B*). These results are consistent with the histochemical observations (Fig. 4*A*). Therefore, breast cancer cells expressing the Runx2 mutant that has lost competency for subnuclear targeting are incapable of blocking osteogenic differentiation. Thus, the TD mutant protein dramatically alters the ability of the parental (MDA-MB-231) breast cancer cell line to modify phenotypic properties of stromal cells.

Requirement of Runx2 Intranuclear Trafficking in Breast Cancer Cells to Form Osteolytic Lesions in Bone. Microarray profiling of a panel of osteogenic genes showed modification in gene expression in the TD-mRunx2 breast cancer cell lines. We compared the parental cells with cells expressing WT or TD-mRunx2. Although expression of many genes was similar among the cell

CELL BIOLOGY

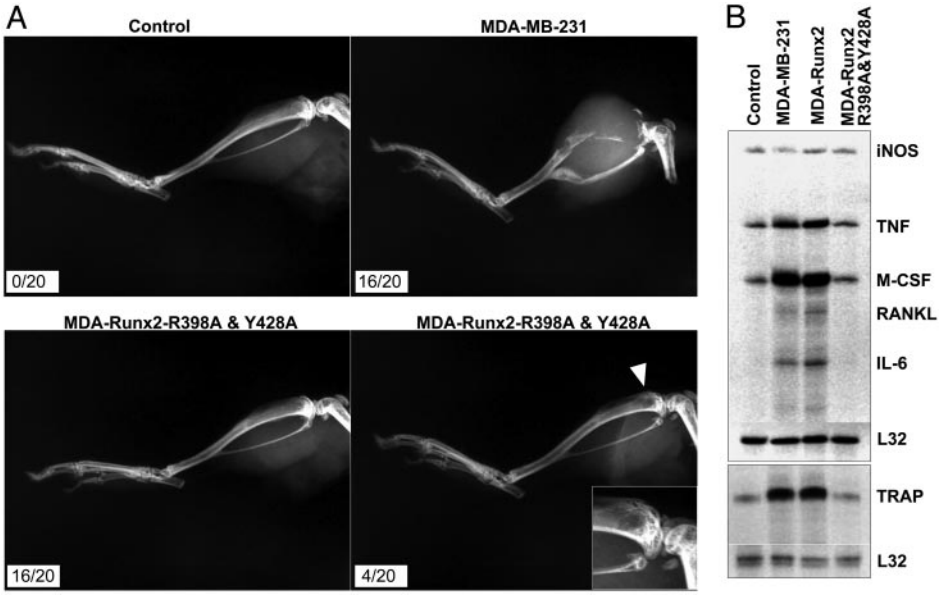

Fig. 6. Subnuclear trafficking of Runx2 is associated with *in vivo* formation of osteolytic lesions by breast cancer cells. (*A*) Control (no cell), MDA-MB-231 parental cell, or targeting-deficient mutant Runx2 (R398A & Y428A) expressing stable cells were injected into the intramedullary region of the tibia of 4- to 6-week-old SCID mice. Formation of osteolytic lesions in bones was assessed by radiography (see text). (*B*) RPA of genes reflecting bone resorbing activity. Total RNA from mouse BMSC and human breast cancer cell cocultures was isolated and probed for mouse osteoclast-related markers, as described in *Materials and Methods*. Markers are as follows: inducible nitrous oxide (iNOS), TNF-α $\kappa\beta$ ligand (RANKL), IL-6, tartrate-resistant acid phosphatase (TRAP) and the internal control ribosomal protein gene (L32). Increased expression of WT Runx2 does not significantly modify gene expression in the parental MDA-MB-231 cells.

lines, a specific subset of genes exhibited alterations (data not shown). Among the genes that are specifically up-regulated by the WT but not the TD mutant is VEGF, a key factor for the invasive process in both bone remodeling and tumorigenesis (37, 38). This pattern of expression was validated by quantitative RT-PCR for VEGF and also for MMP13, a gene highly expressed in metastatic cancer cells (Fig. 5*A*). Compared with the parental MDA-MB-231 cells, both genes were up-regulated (10- to 30-fold) in the WT Runx2 cell line but not in the cell line expressing the mutant Runx2 protein. These studies demonstrate that the TD-mRunx2 protein modifies expression of genes associated with tumorigenic properties (39, 40).

Blocking subnuclear targeting affects the invasive properties of these stable breast cancer cell lines, as determined by the Matrigel assay system (Fig. 5*B*). Expression of WT Runx2 stimulated invasion to 89%, compared with 77% for the parental MDA-MB-231 line, whereas the TD-Runx2 mutant resulted in a significant loss of invasive properties to only 40% (Fig. 5*B*). Thus, our findings indicate that loss of Runx2 subnuclear trafficking alters expression of genes related to both cell migration and invasive properties of breast cancer cells (41, 42).

Breast cancer metastasis to bone characteristically results in osteolytic lesions (43). We have shown (29) that Runx2 activity is a critical determinant for osteolysis. Therefore, we directly addressed the contribution of Runx2 subnuclear targeting to osteolytic bone destruction. The parental MDA-MB-231 breast cancer cells, which expresses Runx2, and the TD-mRunx2 expressing stable cells were locally injected into tibia of immunocompromised mice (see Methods in ref. 29). The parental MDA line resulted in formation of pronounced bone lesions in 80% (16/20) of injected animals as detected by radiographic imaging (Fig. 6*A*). In contrast, MDA cells expressing TD-mRunx2 did not induce lesions in 80% of the injected animals (16/20), and they showed only a few smaller lesions in 20% of the animals (4/20). Thus, the loss of Runx2 association with the nuclear scaffold compromises the ability of breast cancer cells to generate osteolytic lesions in bone *in vivo*.

To gain insight into Runx2 regulated mechanisms of tumor-related bone destruction, we examined genes associated with osteolytic activity by using the coculture system. Cytokines and factors required for formation and activity of osteoclasts are strongly induced in the mouse marrow stromal cells, when cultured with the parental MDA line or with MDA cells expressing WT Runx2 (Fig. 6*B*). However, this induction is prevented by MDA cells expressing the TD-Runx2 mutant protein. Furthermore, we confirmed that tartrate-resistant acid phosphatase a marker of mature osteoclasts, is not induced by the TD-mRunx2 cell line but is induced by both the parental and WT-Runx2 MDA cells (Fig. 6*B*). These results define a pivotal role for Runx2 subnuclear localization in induction of osteoclastic activity by breast cancer cells that metastasize to bone.

Conclusion

Results from numerous studies have shown that tumor cells exhibit disrupted signaling cascades that profoundly alters cell phenotype. Runx transcription factors serve as scaffolds for the assembly of multiprotein complexes and integrate regulatory signals at subnuclear domains. Here, we have shown that a targeting-deficient mutant of Runx2 engages coregulatory protein to form complexes, but the complexes are not targeted to the nuclear matrix scaffold. These findings demonstrate that inhibiting the Runx2 targeting function modifies the phenotype of metastatic breast cancer cells and impairs their tumorigenic and osteolytic activities in bone. As a consequence of altering fidelity of Runx2 intranuclear trafficking, we have modified gene expression in the tumor cell that disrupts the exchange of regulatory signals between the tumor cell and the bone environment. We propose that the Runx2 nuclear matrix targeting module has potential implications for development of therapeutic approaches that disable cancer cell activity.

This work was supported by National Institutes of Health Grants P01AR48818, P01CA82834, R01AR47045, DK32520, R01AR047045, and P01AR0409920.

1. Okuda, T., van Deursen, J., Hiebert, S. W., Grosveld, G. & Downing, J. R. (1996) *Cell* **84,** 321–330.
2. Komori, T., Yagi, H., Nomura, S., Yamaguchi, A., Sasaki, K., Deguchi, K., Shimizu, Y., Bronson, R. T., Gao, Y.-H., Inada, M., *et al.* (1997) *Cell* **89,** 755–764.
3. Li, Q. L., Ito, K., Sakakura, C., Fukamachi, H., Inoue, K., Chi, X. Z., Lee, K. Y., Nomura, S., Lee, C. W., Han, S. B., *et al.* (2002) *Cell* **109,** 113–124.
4. Nucifora, G. & Rowley, J. D. (1995) *Blood* **86,** 1–14.
5. Mundlos, S., Otto, F., Mundlos, C., Mulliken, J. B., Aylsworth, A. S., Albright, S., Lindhout, D., Cole, W. G., Henn, W., Knoll, J. H. M., *et al.* (1997) *Cell* **89,** 773–779.
6. Zeng, C., van Wijnen, A. J., Stein, J. L., Meyers, S., Sun, W., Shopland, L., Lawrence, J. B., Penman, S., Lian, J. B., Stein, G. S., *et al.* (1997) *Proc. Natl. Acad. Sci. USA* **94,** 6746–6751.
7. Zeng, C., McNeil, S., Pockwinse, S., Nickerson, J. A., Shopland, L., Lawrence, J. B., Penman, S., Hiebert, S. W., Lian, J. B., van Wijnen, A. J., *et al.* (1998) *Proc. Natl. Acad. Sci. USA* **95,** 1585–1589.
8. Zaidi, S. K., Javed, A., Choi, J.-Y., van Wijnen, A. J., Stein, J. L., Lian, J. B. & Stein, G. S. (2001) *J. Cell Sci.* **114,** 3093–3102.
9. Tang, L., Guo, B., Javed, A., Choi, J.-Y., Hiebert, S., Lian, J. B., van Wijnen, A. J., Stein, J. L., Stein, G. S. & Zhou, G. W. (1999) *J. Biol. Chem.* **274,** 33580–33586.
10. Capco, D. G. & Penman, S. (1983) *J. Cell Biol.* **96,** 896–906.
11. Nickerson, J. A. & Penman, S. (1992) *Cell Biol. Int. Rep.* **16,** 811–826.
12. Lian, J. B., Javed, A., Zaidi, S. K., Lengner, C., Montecino, M., van Wijnen, A. J., Stein, J. L. & Stein, G. S. (2004) *Crit. Rev. Eukaryot. Gene Expr.* **14,** 1–41.
13. Javed, A., Gutierrez, S., Montecino, M., van Wijnen, A. J., Stein, J. L., Stein, G. S. & Lian, J. B. (1999) *Mol. Cell. Biol.* **19,** 7491–7500.
14. Javed, A., Guo, B., Hiebert, S., Choi, J.-Y., Green, J., Zhao, S.-C., Osborne, M. A., Stifani, S., Stein, J. L., Lian, J. B., *et al.* (2000) *J. Cell Sci.* **113,** 2221–2231.
15. Gutierrez, S., Javed, A., Tennant, D., van Rees, M., Montecino, M., Stein, G. S., Stein, J. L. & Lian, J. B. (2002) *J. Biol. Chem.* **277,** 1316–1323.
16. Paredes, R., Arriagada, G., Cruzat, F., Villagra, A., Olate, J., Zaidi, K., van Wijnen, A. J., Lian, J. B., Stein, G. S., Stein, J. L., *et al.* (2004) *Mol. Cell. Biol.* **24,** 8847–8861.
17. Hassan, M. Q., Javed, A., Morasso, M. I., Karlin, J., Montecino, M., van Wijnen, A. J., Stein, G. S., Stein, J. L. & Lian, J. B. (2004) *Mol. Cell. Biol.* **24,** 9248–9261.
18. Javed, A., Barnes, G. L., Jassanya, B. O., Stein, J. L., Gerstenfeld, L., Lian, J. B. & Stein, G. S. (2001) *Mol. Cell. Biol.* **21,** 2891–2905.
19. Schroeder, T. M., Kahler, R. A., Li, X. & Westendorf, J. J. (2004) *J. Biol. Chem.* **279,** 41998–42007.
20. Zaidi, S. K., Sullivan, A. J., van Wijnen, A. J., Stein, J. L., Stein, G. S. & Lian, J. B. (2002) *Proc. Natl. Acad. Sci. USA* **99,** 8048–8053.
21. Afzal, F., Pratap J., Ito K., Ito Y., Stein J. L., van Wijnen A. J., Stein G. S., Lian J. B. & Javed A. (2004) *J. Cell. Physiol.*, in press.
22. Stein, G. S., Zaidi, S. K., Braastad, C. D., Montecino, M., van Wijnen, A. J., Choi, J.-Y., Stein, J. L., Lian, J. B. & Javed, A. (2003) *Trends Cell Biol.* **13,** 584–592.
23. Choi, J.-Y., Pratap, J., Javed, A., Zaidi, S. K., Xing, L., Balint, E., Dalamangas, S., Boyce, B., van Wijnen, A. J., Lian, J. B., *et al.* (2001) *Proc. Natl. Acad. Sci. USA* **98,** 8650–8655.
24. Zaidi, S. K., Sullivan, A. J., Medina, R., Ito, Y., van Wijnen, A. J., Stein, J. L., Lian, J. B. & Stein, G. S. (2004) *EMBO J.* **23,** 790–799.
25. Kundu, M., Javed, A., Jeon, J. P., Horner, A., Shum, L., Eckhaus, M., Muenke, M., Lian, J. B., Yang, Y., Nuckolls, G. H., *et al.* (2002) *Nat. Genet.* **32,** 639–644.
26. North, T., Gu, T. L., Stacy, T., Wang, Q., Howard, L., Binder, M., Marin-Padilla, M. & Speck, N. A. (1999) *Development (Cambridge, U.K.)* **126,** 2563–2575.
27. O'Keefe, R. J. & Guise, T. A. (2003) *Clin. Orthop.* S100–S104.
28. Mundy, G. R. (2002) *Nat. Rev. Cancer* **2,** 584–593.
29. Barnes, G. L., Hebert, K. E., Kamal, M., Javed, A., Einhorn, T. A., Lian, J. B., Stein, G. S. & Gerstenfeld, L. C. (2004) *Cancer Res.* **64,** 4506–4513.
30. Yeung, F., Law, W. K., Yeh, C. H., Westendorf, J. J., Zhang, Y., Wang, R., Kao, C. & Chung, L. W. (2002) *J. Biol. Chem.* **277,** 2468–2476.
31. Brubaker, K. D., Vessella, R. L., Brown, L. G. & Corey, E. (2003) *Prostate* **56,** 13–22.
32. Fey, E. G., Krochmalnic, G. & Penman, S. (1986) *J. Cell Biol.* **102,** 1654–1665.
33. Li, C. & Wong, W. H. (2001) *Proc. Natl. Acad. Sci. USA* **98,** 31–36.
34. Kuznetsov, S. A., Krebsbach, P. H., Satomura, K., Kerr, J., Riminucci, M., Benayahu, D. & Robey, P. G. (1997) *J. Bone Miner. Res.* **12,** 1335–1347.
35. Gerstenfeld, L. C., Cho, T. J., Kon, T., Aizawa, T., Tsay, A., Fitch, J., Barnes, G. L., Graves, D. T. & Einhorn, T. A. (2003) *J. Bone Miner. Res.* **18,** 1584–1592.
36. Lee, Y., Schwarz, E., Davies, M., Jo, M., Gates, J., Wu, J., Zhang, X. & Lieberman, J. R. (2003) *J. Orthop. Res.* **21,** 62–72.
37. van Kempen, L. C. & Coussens, L. M. (2002) *Cancer Cell* **2,** 251–252.
38. Rafii, S., Lyden, D., Benezra, R., Hattori, K. & Heissig, B. (2002) *Nat. Rev. Cancer* **2,** 826–835.
39. Chirgwin, J. M. & Guise, T. A. (2000) *Crit. Rev. Eukaryotic Gene Expr.* **10,** 159–178.
40. Egeblad, M. & Werb, Z. (2002) *Nat. Rev. Cancer* **2,** 161–174.
41. Gerber, H. P., Vu, T. H., Ryan, A. M., Kowalski, J., Werb, Z. & Ferrara, N. (1999) *Nat. Med.* **5,** 623–628.
42. Ferrara, N., Carver-Moore, K., Chen, H., Dowd, M., Lu, L., O'Shea, K. S., Powell-Braxton, L., Hillan, K. J. & Moore, M. W. (1996) *Nature* **380,** 439–442.
43. Kang, Y., Siegel, P. M., Shu, W., Drobnjak, M., Kakonen, S. M., Cordon-Cardo, C., Guise, T. A. & Massague, J. (2003) *Cancer Cell* **3,** 537–549.
44. Pratap, J., Galindo, M., Zaidi, S. K., Vradii, D., Bhat, B. M., Robinson, J. A., Choi, J.-Y., Komori, T., Stein, J. L., Lian, J. B., *et al.* (2003) *Cancer Res.* **63,** 5357–5362.